PHYSICAL REVIEW B VOLUME 20, NUMBER 2 15 JULY 1979

Resonant scattering of exciton polaritons by LO and acoustic phonons

E. S. Koteles*
Max-Planck-Institut für Festkörperforschung, Stuttgart, West Germany

G. Winterling
Physikalisches Institut 4, Universität Stuttgart, West Germany
(Received 27 November 1978)

A change in the shape of the Raman scattering spectrum in CdS is observed when the exciting laser frequency ω_i is tuned across the A-exciton resonance. When ω_i is below resonance a single LO peak is present in the forbidden Raman spectrum $[x(yy)\bar{x}]$. Under resonance conditions two contributions to the spectrum can be distinguished: (i) narrow peaks whose Raman shifts change with the exciting frequency superimposed on (ii) a broad luminescence band which is stationary in frequency. The narrow peaks are interpreted as acoustic-phonon interbranch exciton-polariton scattering followed by LO phonon emission. Their frequency shifts and shapes are consistent with this explanation when the anisotropy of the piezoelectric acoustic phonon–exciton interaction is included. The sudden appearance of these two phonon modes when the exciting frequency is slightly above the A-exciton frequency can only be understood within an exciton-polariton picture. This picture must also be invoked in order to explain the shape of the broad luminescence band which is the LO replica of the free-exciton luminescence.

I. INTRODUCTION

Resonant Raman scattering (RRS) has been extensively studied in semiconductors. In particular, the frequency dependence of the cross section of "forbidden" RRS by LO phonons has been investigated near the absorption edge.[1,2] In this paper we report changes in the shape of the Raman spectrum when the exciting frequency is tuned through a dipole-allowed free-exciton resonance in a direct-band-gap material. The propagation of electromagnetic waves in this case is modified by the strong exciton-phonon interaction leading to coupled modes,[3] i.e., exciton polaritons. These have a strong dispersion near the transverse exciton frequency. At slightly higher frequencies two polariton modes can propagate simultaneously. New peaks, resulting from interbranch polariton scattering, have been predicted[4] and recently observed in the Brillouin spectrum.[5,6] Here we show that new peaks are also observed in the forbidden Raman spectra near the LO frequency. No significant changes were seen near the "allowed" TO peaks.

Undoped CdS was excited at helium temperatures with a narrow-band cw dye laser at frequencies below the A exciton. When tuning the exciting frequency ω_i close to the transverse exciton frequency, a luminescence band developed, in addition to the usual narrow LO peak. When increasing ω_i beyond the onset frequency, ω_{UP}, of the "inner" polariton branch, new Raman peaks appeared near the LO peak. Their intensities were comparable with that of the LO Raman peak when $\omega_i < \omega_{UP}$, their frequency shifts, however, changed with ω_i. At somewhat higher ω_i only these new peaks[7] are seen; unexpectedly the "original" LO peak is not observable above the luminescence background, the LO replica of the free A-exciton resonance. The evolution of this background as ω_i is tuned across the A-exciton resonance has also been studied. The dispersing Raman peaks are interpreted as two-phonon cascade processes in which polariton scattering by acoustic phonons is followed by LO-phonon scattering. Despite the large exciton mass anisotropy, the two-phonon peaks are very narrow. This behavior is attributed to the pronounced anisotropy of the piezoelectric acoustic phonon-exciton interaction.[8,9]

Recently Permogorov and Travnikov[10] have studied the secondary emission spectrum of CdS in the same frequency region at $T = 77$ K with monochomatic light derived from a white light source. Their frequency resolution (~25 cm^{-1}) and higher temperature, however, did not allow them to detect the fine structure in the vicinity of the LO frequency which is clearly observable in our experiment at helium temperatures. Sidebands in resonant Raman spectra have previously been observed by Yu and Shen[11] in Cu_2O and, as weak features beside a strong LO peak in CdSe.[12] In both experiments the sidebands were interpreted in an exciton picture. Several important features of our results in CdS, however, can be explained only by including the polariton aspect.

II. THEORETICAL CONSIDERATIONS

The energy relaxation of resonantly excited polaritons in pure crystals is via scattering by lat-

tice phonons. Hopfield,[13] Bendow and Birman,[14] and Burstein *et al.*[14] describe these processes in the conventional polariton picture.[15] They find that the Stokes efficiency S for incident polaritons $\omega_i(K_i)$ scattered by type-j phonons $\Omega(q)$ into a final polariton mode $\omega_s(K_s)$ inside the crystal is given by

$$S(\Omega_j)\propto(\bar{n}_j+1)|\langle\Psi_i|\tilde{M}_j|\Psi_s\rangle|^2 v_{gi}^{-1}K_s^2 v_{gs}^{-1}. \quad (1)$$

Here $\bar{n}_j$ is the occupation number of the phonons with frequency Ω_j. The energy dependence of the scattering efficiency is primarily determined by two factors: (a) the square of the scattering matrix element $\tilde{M}_j$ which has to be evaluated between initial and final polariton states Ψ_i and Ψ_s, and (b) a dynamical factor which is proportional to the density of scattered polariton states $(K_s^2 v_{gs}^{-1})$. v_{gi} and v_{gs} refer to the group velocities of incident and scattered polaritons which (in the two-branch model) belong to either the inner or outer polariton branch. These polaritons have a frequency-dependent transmission probability T of transforming into an external photon at the crystal surface.[16]

The exciton polariton interacts with phonons through its exciton content. The exciton-phonon interaction is governed by deformation potential (DP) coupling and coupling through the longitudinal electric field E_L of LO phonons or piezoelectrically active acoustic phonons. The first mechanism produces wave-vector-independent ("allowed") terms in the scattering matrix while the second leads to wave-vector-dependent ("forbidden") matrix elements (intraband-Fröhlich scattering) and wave-vector-independent (allowed) scattering through the linear electro-optic effect in noncentrosymmetric crystals. Close to an exciton resonance forbidden LO scattering has been shown to dominate allowed LO scattering in pure polar crystals like CdS.[1,17]

In a first approximation (neglecting contributions from other bands and excited exciton states), *polariton* scattering due to the intraband-Fröhlich interaction is obtained by computing intraband scattering between *exciton* states in the Wannier approximation. For hydrogenic $1S$ wave functions[18,19] and an isotropic mass the corresponding scattering matrix element M (for intraband-Fröhlich coupling) is given by

$$M(E_L,q)\propto(e/q)(E_L E_L^*)^{1/2}\{[1+(r_h a_0 q)^2]^{-2} - [1+(r_e a_0 q)^2]^{-2}\}, \quad (2)$$

where $r_h=m_h/2(m_e+m_h)$ and $r_e=m_e/2(m_e+m_h)$, m_e and m_h are the effective electron and hole mass, respectively, a_0 is the exciton radius, and q is the wave vector of the scattering phonon. The q-dependent quantities inside the curly brackets are the Fourier transforms of the charge distributions of the electron or hole in the internal motion. They lead, as in the case of the DP interaction, to a decrease of the exciton-phonon interaction at phonon wavelengths $2\pi/q$ smaller than the Bohr radius a_0. For $(ra_0q)^2\ll1$ which corresponds in CdS to $q<a_0^{-1}\simeq3.5\times10^6$ cm^{-1} the q dependence of M in Eq. (2) can simply be described by

$$M(E_L,q)\propto e(E_L E_L^*)^{1/2}a_0^2 q\,\frac{m_h-m_e}{m_h+m_e}. \quad (3)$$

M^2 increases rapidly with increasing q reaching a maximum at $a_0q\sim1.8$. Thus, in comparison to the DP coupling, the strength of the intraband-Fröhlich scattering at small q contains an additional q^2 dependence.

The coupling of pieozoelectrically active acoustic phonons with excitons can be described in a fashion similar to LO-phonon–exciton coupling; in particular the scattering matrix element M has the same form as that of the Fröhlich interaction described in Eq. (2). However, there are two differences which result from the differing properties of the relevant electric fields, E_L. First, M^2 for acoustic phonons has an additional factor q (for acoustic phonons E_L is proportional to the strain while for LO phonons E_L is proportional to the displacement). Second, in wurtzite crystals, such as CdS, the strength of the piezoelectric field E_L^p is a sensitive function of the angle, ϕ, between $\vec{q}$ and the c axis[8] and possesses strong maxima in both symmetry and off-symmetry directions. In contrast, the quasi-LO and -TO frequencies and consequently the electric field E_L^{LO} are weakly dependent on ϕ in CdS.[20] Intraband-Fröhlich coupling involving acoustic phonons has been shown to be responsible for forbidden TA backscattering[21] and narrow two-phonon peaks in the Brillouin spectrum of CdS.[6,22] On the other hand, the angular dependence of DP coupling is much weaker (see the Appendix).

Significant changes have been observed in the resonant Brillouin spectra of[5] GaAs and[6,23] CdS when the exciting frequency ω_i was tuned through the onset frequency ω_{UP} of the inner polariton branch (labeled 1 in Fig. 1). Brillouin lines, seen when $\omega_i<\omega_{UP}$, weakened and a new set of peaks appeared. These changes are intimately related to the transmission properties of the polariton-photon system at the crystal surface. For $\omega_i<\omega_{UP}$ mainly the outer polariton branch (labeled 2 in Fig. 1) is populated while for $\omega_i>\omega_{UP}$ the inner branch is dominantly populated. Therefore, only polaritons of branch 1 have a high probability of transforming into an external photon when $\omega_i>\omega_{UP}$ (The energy transmission coefficient T of the outer branch has been shown to decrease quite rapid-

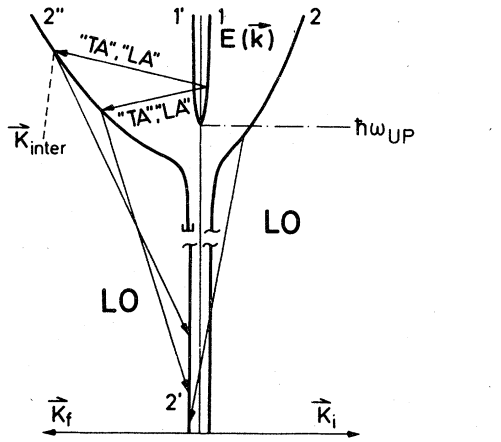

FIG. 1. Schematic exciton polariton dispersion curves in the vicinity of the A exciton in CdS. Possible one- and two-phonon scattering channels are illustrated. While the initial- (branches 1 and 2) and final-state (branch 2′) polaritons propagate with $\vec{K} \perp \vec{c}$ axis, intermediate-state polaritons (branch 2″) propagate in different directions so that the angle $\phi(\vec{K}_{inter}, \vec{c}) \neq 90°$; the dispersion of branch 2″ is determined by a heavier exciton mass due to the mass anisotropy in CdS, $\vec{K}_i$ and $\vec{K}_f$ denote the wave vectors of incident and final-state polaritons.

ly in CdS,[16] for $\omega_i > \omega_{UP}$; details of its frequency variation, however, depend on the choice of the additional boundary condition[24]).

Since the inner and outer branches involve quite different wave vectors significant changes are expected in the forbidden Raman spectrum when ω_i is tuned across ω_{UP}. (No equivalent changes are expected for the allowed Raman spectrum since its efficiency is only weakly dependent on q.) In particular two-step cascade processes involving acoustic phonons become possible (see Fig. 1). Incident polaritons on the inner branch are first scattered by acoustic phonon emission or absorption into large-k intermediate states on the outer branch; these are then scattered by LO emission into photonlike final states. These processes lead to new peaks on either side of the LO emission peak. Their frequency shifts are linked, via the acoustic-phonon wave vector, with the exciton polariton dispersion and, thus, they are dispersive. The spectral shape of these two-phonon bands is obtained by summing the contributions of all intermediate states. If the phonon-exciton coupling is isotropic, these bands should be rather broad in CdS due to the anisotropy of the exciton mass.[10] For example, at $\omega_i = 20\,640$ cm^{-1}, frequency shifts for $(1 \rightarrow 2')$ Stokes scattering range from 3 to 6 cm^{-1} for quasi-TA phonons and from 7 to 13 cm^{-1} for quasi-LA phonons for $\vec{q} \perp \vec{c}$ and $\vec{q} \parallel \vec{c}$, respectively.

III. EXPERIMENT

The undoped, single crystal CdS platelets were grown from the vapor phase and were about 30 μm thick. Samples were selected which exhibited a free-exciton luminescence relatively strong in comparison with bound exciton lines. They were cooled by helium exchange gas down to 6 K in order to reduce the background luminescence resulting from multiphonon processes. The exciting radiation was provided by a cw dye laser employing coumarin 102 pumped with the deep blue lines of a high-power krypton laser (~1 W). It was focused onto the sample with a cylindrical lens resulting in an excitation power density of about 1 W/cm^2. The incident light was directed normal to the face of the platelet which contained the crystallographic c axis. Thus, polaritons propagating with $\vec{K} \perp \vec{c}$ were excited. The backscattered light was collected with an $f/3.5$ lens. After passing through a polarizer it was spectrally analyzed with a standard double grating monochromator employing photon counting detection. The combined spectrometer–dye-laser half-width was about 0.6 cm^{-1}. The Raman shifts were reproducible to within ± 0.3 cm^{-1}; their absolute values, however, were uncertain by ± 1 cm^{-1} due to inaccuracies of the spectrometer drive.

IV. EXPERIMENTAL RESULTS

The secondary emission spectrum of CdS was mainly investigated in a range centered on the longitudinal-optic (LO) phonon frequency (~307 cm^{-1} below ω_i). For incident frequencies ω_i about 20 cm^{-1} below ω_T, the transverse A-exciton frequency, the forbidden scattering spectrum [geometry $x(yy)\bar{x}$ in the standard notation[25]] contained only one narrow Raman peak corresponding to the E_1(LO) phonon with $\omega_{LO} \simeq 307$ cm^{-1} for $q \rightarrow 0$. The allowed LO scattering, observable[20] in $x(zy)\bar{x}$ and $x(yz)\bar{x}$, was weaker by at least a factor of 20.

As ω_i approached ω_T, the character of the spectrum changed; a broad luminescence band (the LO replica of the free-exciton luminescence) appeared and quickly came to dominate the emission spectrum. (See, for example, the spectrum with $\omega_i = 20\,600$ cm^{-1} in Fig. 2, where the narrow Raman peak is superimposed on the broad asymmetric LO replica luminescence.) The peak separation of the free-exciton luminescence and the LO replica was about 298 cm^{-1}, or approximately 9 cm^{-1} less than the LO frequency. The LO peak intensity I_{LO}, uncorrected for absorption or reflection losses, had a maximum at $\omega_i = 20\,585$ cm^{-1}, i.e., slightly below $\omega_T \simeq 20\,589$ cm^{-1}. I_{LO} then decreased and reached a minimum at $\omega_i = 20\,593$ cm^{-1}, which is close to the position of the transmission mini-

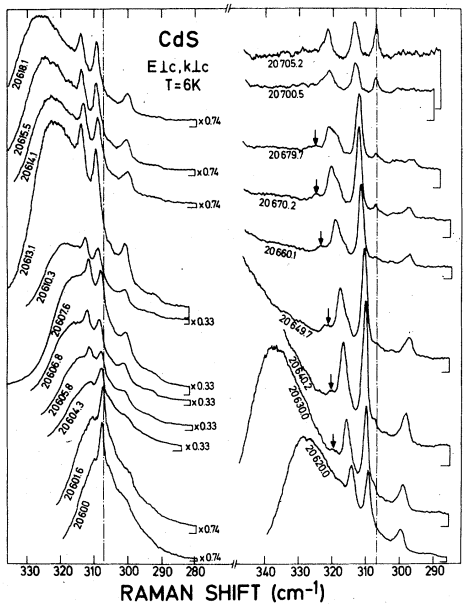

FIG. 2. Emission spectra of CdS excited by a sequence of different incident frequencies ω_i and observed in the scattering geometry $x(yy)\bar{x}$. The values of ω_i are given in wave numbers. The linear vertical scale on the left-hand side is reduced by factors of 0.33 or 0.74. The dash-dotted line marks the position of the LO peak for ω_i below resonance.

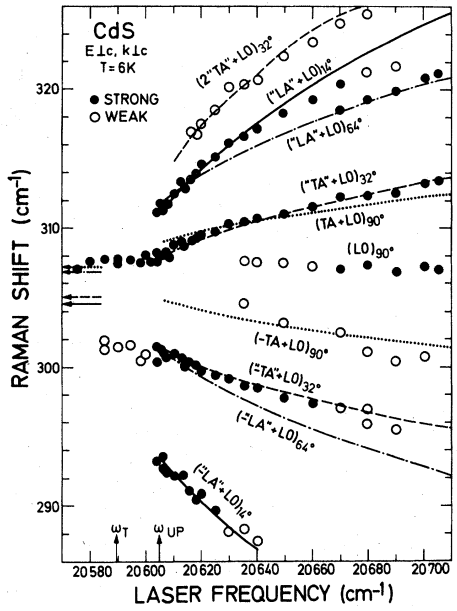

FIG. 3. Measured (circles) and calculated (lines) Raman shifts vs incident frequency. The numbers beside the brackets refer to the angles ϕ between the phonon wave vector $\vec{q}$ and the c axis. The arrows at the left indicate LO frequencies for $q \to 0$ ($\phi = 14°$, 32°, 64°, and 90° in sequence of increasing frequency).

mum of very thin platelets.[26] The intensity of the LO replica luminescence, on the other hand, increased monotonically with ω_i throughout this region.

When ω_i was increased beyond the onset frequency of the inner polariton branch ($\omega_{UP} \simeq 20\,605$ cm^{-1}), the spectral shape near the LO frequency changed dramatically. Several narrow Raman peaks suddenly appeared superimposed on the luminescence background. No significant changes were observed near the TO frequencies. As ω_i was increased further the frequency shifts of all the peaks changed; the two strong peaks increased in frequency while the other two peaks decreased in frequency. Surprisingly no separate Raman peak could be seen at the LO position (~307 cm^{-1}) from about $\omega_i \simeq 20\,610$ cm^{-1} to $\omega_i \simeq 20\,640$ cm^{-1} when a weak feature reappeared. This feature became comparable in intensity to the other Raman peaks only when ω_i was close to the B-exciton frequency (see Fig. 2; $\omega_i = 20\,705.2$ cm^{-1}). Previously Raman sidebands had been observed in CdSe (Ref. 12) which has the same crystal structure as CdS. There are, however, important differences between the spectra of CdSe and those of CdS reported here. First the sidebands in CdSe were weak and broad compared with the strong narrow LO peak; in contrast the new Raman peaks in CdS are strong and relatively narrow. Furthermore, the LO peak was not observable in CdS within a certain frequency range (see Fig. 2). Hence, the expression "sidebands" is not appropriate, in general, for CdS. Finally, the new Raman peaks were observed in CdS over a wide frequency range between the A and B exciton while the sidebands in CdSe were seen only in a limited range around the B exciton.

The dispersion of the Raman shifts as a function of ω_i is summarized in Fig. 3. Here the top curve refers to the weak feature (labeled with arrows in Fig. 2) which appears on the left-hand side of the strong Raman peak. The intensities of the Raman peaks and the LO replica luminescence band both had the same dependence on ω_i for $\omega_i > \omega_{UP}$. First they rapidly increased with ω_i, passed through maxima between 20 620 and 20 630 cm^{-1} and then slowly decreased.

The dispersing Raman peaks exhibited an unusual asymmetry in their polarization characteristics. They were most intense, as expected, in the forbidden scattering polarization yy but could also be seen,[27] weakly, in zy. However, within the limits of the experimental signal to noise, they were absent in yz and zz. The intensity ratio zy/yy of the strongest Raman peak remained constant at about 0.15 for $\omega_{UP} < \omega_i \lesssim 20\,660$ cm^{-1}. Then it began to increase, reaching 0.5 at $\omega_i \simeq 20\,690$ cm^{-1}. The

luminescence background for $\omega_i > \omega_{UP}$ had the same polarization characteristics as the strongest Raman peak.

V. DISCUSSION

A. Intensity of the LO Raman peak

The scattered intensity of the LO peak is determined by the product of the transmission coefficients, the LO scattering matrix elements, and the decay length of the incident polaritons. (The final-state polaritons at frequencies $\omega_f \simeq \omega_T - \omega_{LO}$ suffer practically no damping at helium temperatures.) There are two channels for the 1 LO scattering: first $2 \rightarrow 2'$, the only possible channel when $\omega_i < \omega_{UP}$ and second $1 \rightarrow 2'$, which opens up when $\omega_i \gtrsim \omega_{UP}$. The contribution of channel $2 \rightarrow 2'$ becomes rapidly weaker for $\omega_i > \omega_{UP}$ since most of the incident light energy transfers to the inner branch 1 instead of the outer branch 2.[14,16] The scattering matrix element [intraband-Fröhlich interaction, see Eqs. (2) and (3)] of the $1 \rightarrow 2'$ channel, however, is much smaller than that of channel $2 \rightarrow 2'$ because of the smaller phonon wave vector involved. For example,

$$q^2(1 \rightarrow 2')/q^2(2 \rightarrow 2') \simeq \tfrac{1}{25}$$

at $\omega_i \simeq \omega_{UP}$. Thus the contribution of channel $1 \rightarrow 2'$ is also weak so that a large decrease of the total LO scattering efficiency is expected for $\omega_i > \omega_{UP}$ in the exciton polariton picture. This is in agreement with the observed disappearance of the LO peak (Fig. 2). In impure crystals the effect would be difficult to observe since impurity-induced LO scattering can be comparable to or stronger than intrinsic scattering due to the intraband-Fröhlich interaction.

B. Dispersing two-phonon Raman peaks

We identify the observed dispersing Raman peaks with the two-phonon modes discussed previously. At first sight two features of the data obscure this explanation: (i) the dispersing peaks are narrower than expected and (ii) one of them first appears at the position of the LO Raman peak. These difficulties are resolved when the anisotropies of the properties of CdS are taken into consideration. The narrowing of the dispersing peaks follows naturally if intraband-Fröhlich coupling is assumed to dominate the deformation-potential interaction as pointed out by Yu and Evangelisti[22] (a good assumption for TA scattering but somewhat questionable for LA scattering, see the Appendix). The magnitude of the piezoelectric field E_L depends strongly on the angle ϕ between $\vec{q}$ and the c axis.[8] $|E_L|$ has intense maxima when $\phi = 32°$ (for quasi-TA phonons, "TA") and 0° (LA) and weaker maxima when $\phi = 90°$ (TA) and 64° ("LA"). Thus acoustic phonon scattering due to intraband-Fröhlich coupling is strong only near these four angles. The two-phonon Raman shift $\Delta\omega$ was calculated as a function of ω_i at these angles according to

$$\Delta\omega = \omega_i - \omega_f = \omega_{LO}(\phi) \pm q(\phi)v(\phi). \tag{4}$$

Here the anisotropic exciton mass and phonon velocities v were computed using values[28,29] given in the literature.

The angular dependence of the LO frequency[20] for $\vec{q} \rightarrow 0$ was calculated using its measured values for $\phi = 0$ and $\phi = 90°$. Details of the calculation are given in the Appendix. The resulting theoretical curves, using no adjustable parameters, describe the measured dispersion of the Raman peaks quite well (see Fig. 3). Our interpretation is also supported by the fact that the same dispersing Raman peaks are found in the scattering geometry $z(yy)\bar{z}$ where the incident polaritons propagate with $\vec{k} \parallel \vec{c}$.

It is important to note that the dispersing Raman peaks are first observed when $\omega_i \simeq 20\,605$ cm^{-1}. This is exactly the onset frequency of the inner exciton polariton branch calculated using parameters measured with resonant Brillouin scattering.[6] On the other hand, in an exciton picture, two-phonon Raman modes should first be visible when $\omega_i \simeq \omega_T = 20\,589.5$ cm^{-1}.

Let us now discuss some details of the interpretation. The strong Raman peaks with Stokes shifts larger than $\omega_{LO} \simeq 307$ cm^{-1} are narrower than the peak with the smaller shift (see Fig. 2). This is a consequence of the anisotropy of the properties of CdS. While the LO frequency becomes somewhat larger with increasing angle, the corresponding acoustic-phonon frequency becomes smaller due to the anisotropy of the exciton mass. Thus the two-phonon sum modes, for example, $\omega_{LO} + \omega_{TA}$, are narrowed while the difference modes $\omega_{LO} - \omega_{TA}$ are broadened. In addition the anisotropy of the TA velocity near $\phi \sim 32°$ tends to cancel the effect of the mass anisotropy on $q(\phi)$ so that the frequency $\Delta\omega_{TA}$ remains almost constant over a wide range of intermediate $\vec{q}$ states near $\phi \sim 32°$. The difference peaks are less intense than the sum peaks due to the small occupation number of the relevant acoustic phonons at $T \simeq 6$ K.

A feature peculiar to CdS is the observation that the two-phonon sum peak "TA"+LO (32°) first appears at the position of LO(90°). This is a consequence of the fact that for $\omega_i \sim \omega_{UP}$ the "TA" frequency shift (~3 cm^{-1}) at $\phi \sim 32°$ is approximately compensated by the anisotropy[20] of LO frequency $(\omega_{LO(32°)} - \omega_{LO(90°)} \approx -2.5$ cm^{-1}).

In Fig. 2 the spectra taken at $\omega_i < \omega_{UP}$ (e.g., $\omega_i = 20\,600$ and $20\,601.6$ cm^{-1}) exhibit weak shoulders

at frequency shifts $\Delta\omega_R$ around 301 cm^{-1} which are plotted as open circles in Fig. 3 ($\omega_T \lesssim \omega_i < \omega_{UP}$). The values of $\Delta\omega_R$ also match with a two-phonon process; however here the initial state is not a polariton of the inner but of the outer branch (labeled 2 in Fig. 1). This incident polariton is first scattered by the absorption of a "TA" phonon into intermediate polariton states with ϕ centered around ~32°. An additional scattering process by LO emission leads to the observed final polariton state. The corresponding process in which a "TA" phonon is emitted produces a feature with a frequency shift close to the strong LO Raman peak making it difficult to distinguish in experiment.

Two-phonon scattering can be used to check exciton dispersion at very large wave vectors which are not accessible by studying one-phonon Brillouin scattering.[5,6] The calculated curves in Fig. 3 are based on a parabolic exciton dispersion with mass values derived at small k values, $k \leq 3\times10$ cm^{-1}, and on a linear acoustic-phonon dispersion. The fact that the data for "TA"+LO (32°) scattering are well fitted up to $\omega_i \simeq 20\,710$ cm^{-1} demonstrates that the parabolic approximation is a good description up to $k \simeq q_{TA} \simeq 8.3\times10^6$ cm^{-1}. Here the phonon wave vector q is already larger than the reciprocal Bohr radius a_0 (i.e., $q_{TA}a_0 = 2.3$) and is about $\frac{1}{6}$ of the Brillouin-zone value. For comparison K_{max} in the z direction[30] is $\pi/c \simeq 4.7\times10^7$ cm^{-1}. The data for LA+LO (14°) scattering show a weakening when $\omega_i > 20\,660$ cm^{-1} while those for LA+LO (64°) pick up relative strength. This observation, which is not completely understood, is thought to be related to the q dependence of the scattering matrix elements. At a given ω_i, wave vectors of the various scattering modes are unequal. Thus their q-dependent intensities are also unequal. Further, the mixing of A- and B-exciton bands at large K for $\vec{K} \perp \vec{c}$ is stronger at $\phi = 64°$ than at ϕ ~14°. This also affects the scattering intensities.

The asymmetric polarization characteristics of the dispersing Raman peaks [observed only in $x(yy)\bar{x}$ and $x(zy)\bar{x}$ as described previously] are related to the polarization properties of the A and B excitons in CdS. While the A exciton is dipole active only for $\vec{E} \perp \vec{c}$, i.e., y polarization, the B exciton is active both for $\vec{E} \perp \vec{c}$ and $\vec{E} \parallel \vec{c}$, i.e., y and z polarization.[31] Thus for ω_i near ω_T^A, polaritons are strongly excited only when $\vec{E}_i \perp \vec{c}$, but with increasing ω_i, as the B exciton is approached, they can also be excited with $\vec{E}_i \parallel \vec{c}$. The intermediate polariton state on the outer branch, which may have an admixture of the B exciton depending on the angle $(\vec{K}, \vec{c})$, has predominantly A-exciton character. Since forbidden LO scattering is intraband and the final polariton state also has a dominant A-exciton contribution, scattered light is observed only with $\vec{E}_s \perp \vec{c}$, i.e., y polarization. This reasoning implies that the LO peak, which has no intermediate polariton state, should be observable in the forbidden scattering geometry, i.e., $\vec{E}_s \parallel \vec{E}_i$. Indeed for incident frequencies ω_i near the B excitation the LO peak is observed only in $x(yy)\bar{x}$, but not in $x(zy)\bar{x}$ as are the dispersing two-phonon peaks. For ω_i above the B-exciton frequency, the LO peak is also seen in $x(zz)\bar{x}$.

C. Multiple-acoustic-phonon scattering and the LO replica of the free-exciton luminescence

The character of the secondary emission spectra changes dramatically in the LO region when ω_i is tuned through the free-exciton resonance. The narrow LO peak, observed below resonance (but with ω_i above the bound exciton lines) transforms into a more complex spectrum with two contributions[32] (see Fig. 2 when $\omega_i \gtrsim 20\,615$ cm^{-1}): (i) narrow two-phonon Raman peaks whose frequencies change with the incident frequency ω_i; (ii) a broad background band whose peak position remains approximately stationary (in absolute frequency). This is typical luminescence behavior.

The dual nature of the emission spectra is related to the different intrinsic scattering channels taken by the excitonlike polaritons in the intermediate state [labeled with M in Fig. 4(a)]: (a) intra-

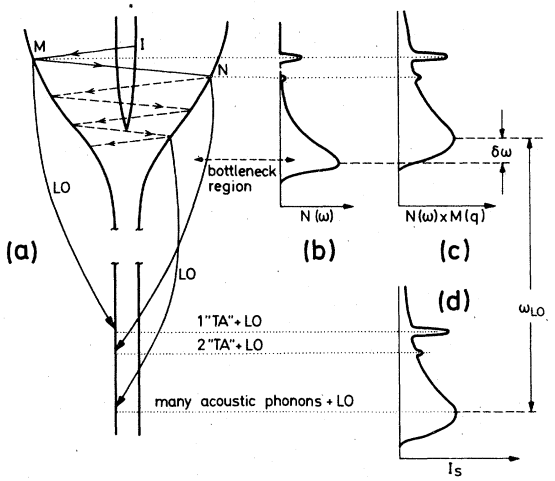

FIG. 4. (a) Schematic of the decay processes of the initial polariton state I with emission of TA phonons and one LO phonon. The spectral density $N(\omega)$ of the occupied polariton states on the outer branch which is observed as free-exciton luminescence is presented in (b). $N(\omega)$ multiplied with the q-dependent matrix element $M(q)$ of the intraband Fröhlich scattering is given in (c). The resulting observed emission spectrum I_s, plotted schematically in (d), has three characteristic features: a broad asymmetric peak representing the LO replica of the free-exciton luminescence and two narrower peaks arising from two-phonon and three-phonon scattering processes.

branch scattering by the emission of one LO phonon giving rise to the dispersing two-phonon Raman peaks, (b) interbranch scattering by acoustic phonons (to the inner polariton branch) observable as dispersing two-phonon Brillouin lines,[6, 22] (c) intrabranch scattering by acoustic phonons. Process (c) leads through multiple-acoustic-phonon scattering (denoted by the dashed lines in Fig. 4) to an accumulation of polaritons in the "knee" of the polariton dispersion curve where the acoustic-phonon scattering rate is slowed down[19] (bottleneck region). Here the relative probability of reaching the crystal surface and transforming into an external photon is increased giving rise to free-exciton luminescence.[19,33]

The second step of the acoustic-phonon cascade, involving scattering from state M to N on the outer branch (see Fig. 4), can be seen in the secondary emission spectra. It corresponds to the weak, dispersing feature with the largest Stokes shift (labeled with arrows in Fig. 2; spectra with $\omega_i > 20\,630$ cm^{-1}); its frequency shift 2"TA"+LO (32°) is plotted in Fig. 3 as the top curve.

The integrated strength of the luminescence band is much larger than that of the dispersing two-phonon modes (see Fig. 2). Thus the acoustic-phonon scattering rate, within the investigated frequency range, must dominate the LO scattering rate. This conclusion is consistent with an earlier finding[21] that the one-phonon Brillouin peaks in CdS are stronger than the LO Raman peak near resonance. However, it is contrary to the behavior generally found in scattering studies of hot electrons.[34] One reason for this difference is that the intraband LO scattering of excitons, in contrast to electron scattering, vanishes for $q \to 0$.[19] This conclusion is concerned with the scattering rate and not with the energy relaxation rate. Theoretical comparisons of LO and LA scattering rates[35] (the latter was only computed for the DP interaction) are compatible with this conclusion.

Raising the sample temperature up to liquid-nitrogen temperatures increases the acoustic-phonon scattering rate [see Eq. (1)] while the LO scattering rate ($\hbar\omega_{LO}/K_b \gg 80$ K) remains essentially constant. Thus, at higher temperatures the two-phonon peaks should lose weight in favor of the luminescence band. This is indeed observed and explains why it is more difficult in pure crystals to observe two-phonon modes at nitrogen temperatures.

The LO replica can be viewed as a probe which maps out the energy distribution of polaritons. Unlike free-exciton luminescence, LO scattering probes polaritons throughout the crystal[33] since the spatial damping of LO scattered polaritons is very weak. Specifically, the intensity distribution of the LO replica reproduces the polariton population (predominantly of the outer branch) integrated over all $\vec{q}$ directions and modulated by the $\vec{q}$ dependence of the Fröhlich matrix element. This $\vec{q}$ dependence is primarily responsible for the reduced frequency separation $\Delta\omega_L$ between the peaks of the LO replica and the free-exciton luminescence; $\Delta\omega_L$ is found to be about $\delta\omega \simeq 8$ cm^{-1} less than the average LO frequency, $\langle\omega_{LO}\rangle \sim 306$ cm^{-1} as illustrated in Fig. 4. This figure also includes a schematic of the polariton population $N(\omega)$. The peaks at states M and N can be viewed as emission by "hot" polaritons while the smoother distribution at the bottleneck reflects "quasithermalized" polaritons.

VI. SUMMARY

We have studied the secondary emission spectrum of CdS in the LO frequency region when the incident frequency ω_i is tuned across the free-exciton resonance. Above resonance two contributions to the spectrum can be distinguished: dispersing Raman peaks and a luminescence background band. While the former arises from *single-acoustic-phonon* scattering followed by LO emission, the luminescence band involves *multiple-acoustic-phonon* scattering followed by LO emission. A polariton description, instead of an exciton picture, is required to explain the onset frequencies of the dispersing Raman peaks, their frequency dispersion close to resonance as well as the sudden disappearance of the LO peak above the onset frequency of the inner polariton branch. This disappearance is attributed to the excitation properties of the polariton branches in conjunction with the q dependence of the intraband Fröhlich interaction and is consistent with the conclusion that the dominant intrinsic damping mechanism of the inner polariton branch[35,36] is acoustic phonon and not LO scattering.

Finally, we comment on the possibility of observing dispersing two-phonon peaks in other polar semiconductors which have a direct band gap, for example, GaAs. The strength of these peaks relative to the luminescence background depends primarily on the ratio of LO-phonon to acoustic-phonon scattering rates (of outer branch polaritons). In general LO scattering[37] and consequently two-phonon peaks will be stronger the more pronounced the polar character of the material. Thus CdS, and other II-VI compounds are good candidates while it should be difficult to observe these peaks above the luminescence background in GaAs.[38]

ACKNOWLEDGMENTS

The authors benefited from discussions with M. Cardona, L. Genzel, J. Lagois, U. Rössler, and P. Y. Yu. They would like to thank Dr. L. Greene of Wright-Patterson Air Force Base, Ohio and Dr. R. Broser of the Fritz-Haber Institute, Berlin for providing the high-quality CdS platelets.

APPENDIX

The frequency shifts, $\Delta\omega$, of the dispersing two-phonon modes in CdS were computed on the following bases:

(i) The relevant LO frequencies are independent of $|\vec{q}|$ and so the dispersion of $\Delta\omega$ arises solely from acoustic-phonon scattering. However ω_{LO} does have an angular dependence given by[20]

$$\omega_{LO}(\phi)=[(\omega_{A_1}\cos\phi)^2+(\omega_{E_1}\sin\phi)^2]^{1/2}, \tag{A1}$$

where ϕ is the angle between the c axis and the phonon wave vector $\vec{q}$ and

$$\omega_{A_1}=\omega_{LO}(0^\circ),\quad \vec{q}_{LO}\parallel\vec{c}$$

$$\omega_{E_1}=\omega_{LO}(90^\circ),\quad \vec{q}_{LO}\perp\vec{c}$$

are experimentally measured.

(ii) The wave-vector-dependent Fröhlich and piezoelectric coupling dominate the deformation-potential coupling.

(iii) Only in K-space directions in which the piezoelectric acoustic-phonon–exciton coupling is strong is there significiant two-phonon scattering. The mean longitudinal electric field associated with a sound wave is proportional to an effective piezoelectric constant[8] $e_{\rm eff}(\phi)$ and to the mean strain S_0.

$$\langle E_L E_L^*(\phi)\rangle=\left(\frac{e_{\rm eff}(\phi)}{\epsilon_0\epsilon_{r0}(\phi)}\right)^2\langle S_0 S_0^*\rangle\,. \tag{A2}$$

Here ϵ_0 is the permittivity of free space and ϵ_{r0} is the static dielectric constant, whose weak angular dependence is neglected. For quasi-"TA" and quasi-"LA" phonons the effective piezoelectric constant has been shown[8] to be

$$e_{\rm eff}(\text{"TA"})=(e_{33}-e_{31}-e_{15})\cos^2\phi\sin\phi+e_{15}\sin^3\phi,$$

$$e_{\rm eff}(\text{"LA"})=e_{33}\cos^2\phi+(e_{31}+2e_{15})\cos\phi\sin^2\phi, \tag{A3}$$

where

$$e_{33}=0.49\ \text{C/m}^2,$$

$$e_{31}=-0.25\ \text{C/m}^2,$$

$$e_{15}=-0.21\ \text{C/m}^2.$$

$e_{\rm eff}^2$ has strong maxima at $\phi=0^\circ$(LA) and $\phi=32^\circ$("TA") and weaker maxima at 64°("LA") and 90°(TA). Since the density of intermediate exciton states (at equal $|\vec{q}|$) approaches zero for $\phi\to0^\circ$, the effective position of the strong LA coupling is shifted from 0° to ~14°.

The frequency shifts $\Delta\omega_A$ of acoustic-phonon scattering (1→2″) were determined for the four maxima:

$$\Delta\omega_A=\pm v(\phi)\,q(\phi).$$

The angularly dependent sound velocity $v(\phi)$ was computed from the known elastic constants[29] and $q(\phi)$ was determined by using the anisotropic exciton polariton dispersion

$$\frac{c^2k^2}{\omega^2}=\epsilon_r\left(1+\frac{\omega_{UP}^2-\omega_T^2}{\omega_T^2+\hbar\omega_T k^2/M_E-\omega^2}\right), \tag{A4}$$

with c the vacuum velocity of light, $\omega_T=20\,589.5$ cm^{-1} the transverse A-exciton frequency, $\omega_{UP}=\omega_T=15.4$ cm^{-1} the longitudinal-transverse exciton splitting, $\epsilon_r=9.3$ the background dielectric constant, M_E the anisotropic exciton mass[22,23] given by

$$M_E=\left(\frac{\sin^2\phi}{m_\perp}+\frac{\cos^2\phi}{m_\parallel}\right)^{-1},$$

where $m_\perp=0.89m_e$ and $m_\parallel=2.8m_e$. The theoretical shifts $\Delta\omega=\omega_{LO}(\phi)\pm v(\phi)q(\phi)$ were calculated using no adjustable parameters. Figure 3 illustrates the good agreement with the experimental data points.

The narrowing of the two-phonon peaks is understood as meaning that acoustic-phonon scattering via the piezoelectric interaction is stronger than that via the DP interaction[22] for the maxima directions when $|q|\geq2.5\times10^6$ cm^{-1}. This assumption is certainly valid for TA scattering since the weak DP interaction is allowed only for off-symmetry directions. Furthermore it was shown experimentally in CdS (Ref. 21) that forbidden TA scattering [via the piezoelectric (PE) interaction] becomes larger than allowed LA scattering (DP interaction) at $\phi=90^\circ$. For this case the ratio of scattering matrix elements evaluated between s-like exciton states is obtained from Eq. (3) in the limit $(a_0q)^2\ll1$.

$$R=\frac{|\langle M^{\rm PE}(\text{TA})\rangle|^2}{|\langle M^{\rm DP}(\text{LA})\rangle|^2}=\left(\frac{ee_{15}q_{\rm TA}a_0^2}{2\epsilon_0\epsilon_{r0}(C_2+C_4)}\,\frac{m_e-m_h}{m_e+m_h}\right)^2\times\frac{v_{\rm LA}}{v_{\rm TA}}\frac{n_{\rm TA}+1}{n_{\rm LA}+1}, \tag{A5}$$

with $a_0=2.8\times10^{-9}$ m the exciton radius, $\epsilon_0=8.85\times10^{-12}$ C V^{-1} m^{-1} the permittivity of free space, $\epsilon_{r0}=9$ the static dielectric constant, $C_2+C_4=1.6$ eV the deformation potential[37], $m_h=m_{h_\perp}=0.7m$ the hole mass[6], $m_e=m_{e_\perp}=0.2m$ the electron mass[31],

$v_{LA}=4.25\times10^5$ cm s^{-1} the longitudinal sound velocity,[29] $v_{TA}=1.76\times10^5$ cm s^{-1} the transverse sound velocity[29], and n_{TA} and n_{LA} the thermal occupation numbers of the corresponding phonons at $T=6$ K. For $q_{TA}=2\times10$ cm^{-1}, which corresponds to $\omega_i\simeq20\,592$ cm^{-1}, $R=1.8\pm0.6$ which is in rough agreement with the experimental ratio[21] (uncorrected for frequency dependent absorption) of 1.0 ±0.3.

On the other hand it is not clear from the available DP data whether the piezoelectric interaction is stronger than the DP interaction for LA scattering. Both the piezoelectric and the DP interactions have their maximum strengths in CdS at $\phi=0°$. Using Eq. (2) the ratio R_{LA} of piezoelectric scattering to DP scattering (for $\vec{q}\|\vec{c}$) is

$$R_{LA}=\frac{\langle M^{PE}(LA)\rangle^2}{\langle M^{DP}(LA)\rangle^2}=\left(\frac{ee_{33}}{\epsilon_0\epsilon_{r0}C_{eff}(q)}\,\frac{f(q)}{q}\right)^2, \tag{A6}$$

where

$$f(q)=[1+(r_h a_0 q)^2]^{-2}-[1+(r_e a_0 q)^2]^{-2}. \tag{A7}$$

$q^{-1}f(q)$ increases linearly with small q and reaches a maximum near $q\simeq2a_0^{-1}=7.12\times10^6$ cm^{-1}.

$C_{eff}(q)$ is the effective deformation potential, which, in general, is also q dependent.[19] In the limit of small q $[(\frac{1}{2}a_0q)^2\ll1]$, $C_{eff}=C_1+C_3=4.1$ eV.[39] The ratio, R_{LA} is evaluated when $q_{LA}=a_0^{-1}=3.57\times10^6$ cm^{-1} (near $\omega_i\simeq20\,610$ cm^{-1}) where the q dependence of C_{eff} can still be neglected. Inserting $m_h=\sqrt{m_{h\perp}m_{h\parallel}}=1.36m$ and $m_e=0.2m$, $R_{LA}=1.17\pm0.47$ with the uncertainty arising mainly from the values of the deformation potential. We note here that exciton scattering by LA phonons via the piezoelectric interaction is smaller than the corresponding electron scattering so that, in contrast to the electron case,[40] exciton scattering via the DP interaction is not negligible relative to that via the piezoelectric interaction.

In the interpretation of the frequency shift of the two-phonon peak, the angular dependence of the effective exciton–LA-phonon interaction is more relevant than the assumed dominance of the piezoelectric interaction. Since the DP interaction also has a maximum for $\vec{q}\|\vec{c}$ axis ($\phi=0°$) and falls off with increasing angle ϕ (however less rapidly than the piezoelectric interaction) it also yields a narrowing of the two-phonon line with emphasis on q directions close to $\phi\sim14°$.

*Present address: Physics Dept., City College, C. U. N. Y., New York 10031.

[1]R. M. Martin and T. C. Damen, Phys. Rev. Lett. 26, 86 (1971); J. M. Ralston, R. L. Wadsack, and R. K. Chang, *ibid.* 25, 814 (1970).

[2]For a review see R. Martin and L. Falicov, in *Light Scattering in Solids*, edited by M. Cardona (Springer, Berlin, 1975), p. 79.

[3]J. J. Hopfield, Phys. Rev. 112, 1555 (1958); J. J. Hopfield and D. G. Thomas, *ibid.* 132, 563 (1963).

[4]W. Brenig, R. Zeyher, and J. Birman, Phys. Rev. B 6, 4617 (1972).

[5]R. G. Ulbrich and C. Weisbuch, Phys. Rev. Lett. 38, 865 (1977).

[6]G. Winterling and E. S. Koteles, in *Proceedings of the International Conference on Lattice Dynamics, Paris, 1977,* edited by M. Balkanski (Flammarion Sciences, Paris, 1978), p. 170.

[7]A preliminary account of this work was reported by E.S. Koteles and G. Winterling in *Physics of Semiconductors, 1978,* edited by B. L. H. Wilson (Institute of Physics, London, 1978), p. 481.

[8]A. R. Hutson, J. Appl. Phys. Suppl. 32, 2287 (1961).

[9]G. D. Mahan and J. J. Hopfield, Phys. Rev. Lett. 12, 241 (1964).

[10]S. Permogorov and V. Travnikov, Phys. Status Solidi B 78, 389 (1976).

[11]P. Y. Yu and Y. R. Shen, Phys. Rev. Lett. 32, 939 (1974).

[12]P. Y. Yu, Solid State Commun. 19, 1087 (1976).

[13]J. J. Hopfield, Phys. Rev. 182, 945 (1969).

[14]B. Bendow and J. L. Birman, Phys. Rev. B 1, 1678 (1970); E. Burstein, R. Ito, A. Pinczuk, and S. Shand, J. Acoust. Soc. Am. 49, 1013 (1971).

[15]R. Zeyher, C. S. Ting, and J. L. Birman [Phys. Rev. B 10, 1725 (1974)] give a new treatment of the polariton theory of Raman scattering. Their results imply that the density of final polariton states in Eq. (1) should be replaced by the external photon density of states. Our results on the frequency dependence of the scattering efficiencies, however, indicate that the group velocity of the final polariton state (inside the crystal) must be included in order to understand the measured frequency dependence; G. Winterling and E. S. Koteles (unpublished).

[16]S. A. Permogorov and A. V. Sel'kin, Fiz. Tverd. Tela 15, 3025 (1973) [Sov. Phys. Solid State 15, 2015 (1974)]; A. Sel'kin, Phys. Status Solidi B 83, 47 (1977).

[17]R. H. Callender, S. S. Sussman, M. Selders, and R. K. Chang, Phys. Rev. B 7, 3788 (1973).

[18]A. I. Anselm and In. A. Firsov, Zh. Eksp. Teor. Phys. 30, 719 (1956) [Sov. Phys. JETP 3, 564 (1956)].

[19]Y. Toyozawa, Prog. Theor. Phys. 20, 53 (1958).

[20]See, for example, C. A. Arguello, D. L. Rousseau, and S. P. Porto, Phys. Rev. 181, 1351 (1969).

[21]G. Winterling, E. S. Koteles, and M. Cardona, Phys. Rev. Lett. 39, 1286 (1977).

[22]P. Y. Yu and F. Evangelisti, Solid State Commun. (to be published).

[23]G. Winterling and E. S. Koteles, Bull. Am. Phys. Soc. 23, 247 (1978).

[24]R. Zeyher, J. L. Birman, and W. Brenig, Phys. Rev.

B 6, 4613 (1972); V. M. Agranovich and V. I. Yudson, Opt. Commun. 7, 121 (1973).

[25]In this notation the letters inside the parentheses refer to the polarization and those outside to the propagation directions of the incident and scattered light, respectively; $\vec{z} \| \vec{c}$ axis.

[26]J. Voigt, Phys. Status Solidi B 64, 549 (1974); J. Voigt, M. Senoner, and I. Rückmann, Phys. Status Solidi B 75, 213 (1976).

[27]A similar polarization dependence was found in CdSe, see Ref. 12.

[28]See Refs. 6 and 23 for the effective mass of the exciton.

[29]D. Gerlich, J. Phys. Chem. Solids 28, 2575 (1967).

[30]The lattice constant $c = 6.72$ Å; see W. L. Roth, in *Physics and Chemistry of II-VI Compounds*, edited by M. Aven and J. S. Prener (North-Holland, Amsterdam, 1967), p. 128.

[31]D. G. Thomas and J. J. Hopfield, Phys. Rev. 116, 573 (1959).

[32]A transformation from Raman scattering to photoluminescence at the C exciton of CdSe has been observed by P. Y. Yu and J. E. Smith [Phys. Rev. Lett. 37, 622 (1976)].

[33]H. Sumi, J. Phys. Soc. Jpn. 41, 526 (1976).

[34]See, for example, R. G. Ulbrich, Solid State Electron. 21, 51 (1978); H. J. Stocker and H. Kaplan, Phys. Rev. 150, 619 (1966).

[35]A. A. Demidenko, Fiz. Tverd. Tela 5, 2835 (1963) [Sov. Phys. Solid State 5, 2074 (1964)]; W. C. Tait and R. L. Weither, Phys. Rev. 178, 1404 (1969).

[36]F. Spiegelberg, E. Gutsche, and J. Voigt, Phys. Status Solidi B 77, 233 (1976).

[37]The LO scattering rate depends not only on the scattering matrix element M evaluated between exciton states [see Eq. (2)] but also on the exciton amplitude of the final polariton state ψ_s [see Eq. (1)]. This amplitude is a function of the oscillator strength of the exciton transition (see Ref. 13), which is a reflection of the polar character of the material. Since the LO frequency of GaAs is comparable with that of the A_1 and E_1 LO phonons in CdS and since, on the other hand, the exciton oscillator strength in GaAs is about an order of magnitude weaker than in CdS, the LO scattering should be stronger in CdS than in GaAs. Moreover the density of final polariton states also favors CdS. In acoustic-phonon scattering the final polariton state is always close to resonance so that the polariton wave function is practically excitonlike and its exciton amplitude is close to unity.

[38]No two-phonon Raman line superimposed on the LO replica luminescence has yet been observed in GaAs; C. Weisbuch and R. Ulbrich, J. Lumin. (to be published).

[39]D. W. Langer, R. N. Euwema, K. Era, and T. Koda, Phys. Rev. B 2, 4005 (1970); V. B. Sandomirskii, Fiz. Tverd. Tela 6, 324–326 (1964) [Sov. Phys. Solid State 6, 261 (1965)].

[40]S. S. Devlin, in *Physics and Chemistry of II-VI Compounds*, edited by M. Aven and J. S. Prener (North-Holland, Amsterdam, 1967).